Cardiac Cell Networks on Elastic Microgrooved Scaffolds

HAROLD BIEN, LIHONG YIN,
AND EMILIA ENTCHEVA

Major initiatives are underway to create implantable engineered heart constructs for repair of damaged myocardium [1], but integration of such engineered patches of heart muscle with the injured heart will require deeper understanding of the interactions between cardiomyocytes in networks of cells. Furthermore, while many engineered cardiac constructs lack preferential cell orientation, the actual in vivo heart tissue is structurally and functionally anisotropic [2]. Therefore, we sought to construct a model-engineered cardiac construct having anisotropic properties and consisting of inter-connected cardiac cells with syncytial tissue-like behavior. We report basic structural, electrophysiological and mechanical characterization of multicellular tissue-like engineered constructs developed using elastic matrices with 3-D surface microtopography. To properly assess functionality of the constructs in the tissue setting, we employed spatial optical fluorescence techniques enabling measurements at the micro- and macro-scale.

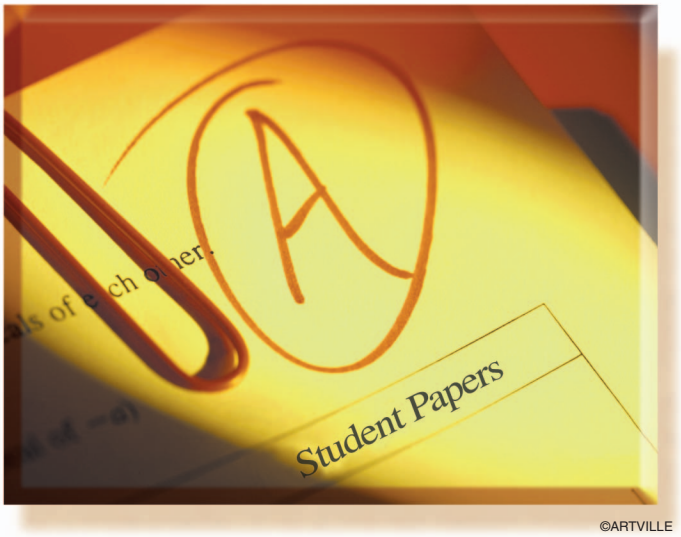

©ARTVILLE

Methods

Cell Culture and Scaffolding

Neonatal cardiomyocytes were isolated and cultured as previously described [3]. Briefly, ventricles of 3-day-old rats were digested with trypsin (Invitrogen, Carlsbad, California) and collagenase (Worthington, Lakewood, New Jersey) before plating at 4.7×10^5 cells/cm^2 on fibronectin-coated scaffolds and kept at 37 °C in a CO_2 incubator in medium M199 supplemented with 2% fetal bovine serum (Invitrogen). Cells were grown either on elastic microgrooved scaffolds (G) or control flat surfaces (F). Microgrooved scaffolds were prepared using acoustic micromachining [4]. In short, we molded polydimethylsiloxane (PDMS from Dow Corning, Midland, Michigan) from a master template, prepared using phonograph record technology; control flat surfaces were made by pouring PDMS on a smooth surface. The surface topography was chosen to consist of deep (50 μm) trapezoidal grooves, separated by triangular ridges about 120 μm apart to provide quasi 3-D microenvironment with cell-compatible feature dimensions. PDMS was selected as a scaffold material because of its biocompatibility, elasticity, optical clarity, and lack of autofluorescence.

Immunocytochemistry

To examine structural differences between F and G scaffolds, at day seven of culture the cell constructs were fixed in 3.7% formaldehyde and stained for F-actin using phalloidin conjugated to Alexa-488 (Molecular Probes, Eugene, Oregon) or for connexin-43 (Cx43) using rabbit anti-mouse Cx43 (Chemicon, Temecula, California) and goat anti-rabbit antibodies conjugated to Alexa-488 (Molecular Probes). Immunofluorescence images were collected using a scanning laser confocal microscope, BioRad Radiance 2000, with a 60x oil-immersion objective (N.A. 1.4) having vertical resolutions of 0.5-1 μm. Quantification of gap junction size and density from optical confocal slices was done by *granulometry* using the Image Processing Toolbox in MATLAB (Mathworks, Natick, Massachusetts). Morphological operations were used to find objects close in size to a chosen structural element (test pattern). Dividing the number of pixels found by the area of the structural element then estimates the number of clusters having the same area as the structural element without individually enumerating each cluster.

Editor's Note: This article won first place in the 2002 EMBS Student Paper Competition. Except for minor editing and formatting changes, the article appears as it was submitted for the competition.

 0739-5175/03/$17.00©2003IEEE

Functionally, the engineered constructs exhibited extreme levels of anisotropy, which could be well controlled in our system by the spatial features in the master template.

Electromechanical Characterization

Microscopic electrophysiological and mechanical comparison of F and G scaffolds were performed by a dual-sensor fluorescence setup (using an inverted microscope), schematically shown in Figure 1 (Ionoptix, Milton, Massachusetts). The system permits simultaneous fluorescence measurements of electrical activity in epi-illumination mode and bright-field imaging of mechanical motion in trans-illumination. The area of measurements was aperture-limited to only a few cells. Intracellular calcium was measured using the calcium-sensitive dye Fura-2 (Molecular Probes) and a dual-excitation ratiometric fluorescence technique to avoid problems with dye loading and to enable quantification. Cell length (for strain calculations) was recorded simultaneously via trans-illumination by computer-assisted software tracking of cell edges or other naturally occurring high contrast features. Calcium-related fluorescence data were acquired at 1 kHz with a photomultiplier tube (PMT), while cell length changes were sampled at 0.24 kHz with a charge-coupled device (CCD) camera. Experiments lasting 20-60 minutes were typically conducted in pairs (F and G scaffolds), stained simultaneously with 5 μM Fura-2 AM and perfused throughout with warm (30-32 °C) Tyrode's solution. Electric field stimulation was applied through built-in Pt electrodes in the side walls of the perfusion chamber.

Experimental data were filtered and analyzed to extract quantitative information; i.e., to determine systolic calcium

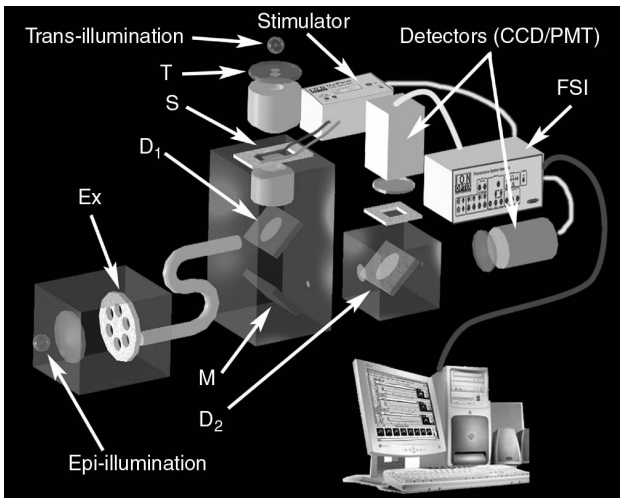

Fig. 1. Schematic diagram of a microscopic system for simultaneous dynamic fluorescence measurements and mechanical analysis. Epi-illumination light is supplied by a xenon arc-lamp and is filtered through one of several possible excitation filters (Ex) on a filter wheel before reflecting off the first dichroic mirror (D_1, long-pass 400 nm) and illuminating the specimen (S). Simultaneously, an incandescent lamp trans-illuminates the sample through a 665-nm filter (T). This transmitted light passes through the sample, D_1, and a second dichroic mirror D_2 (586-nm long pass) and enters the CCD camera for mechanical motion analysis. Fluorescence emitted from the specimen also passes through D_1 but reflects off D_2 and is collected by a photo-multiplier tube (PMT) with an emission filter at 510 nm. Internal plain mirrors redirect light through the optical pathways of the microscope and are represented schematically by M. The detectors and the filter wheel are computer-controlled through the Fluorescence System Interface (FSI).

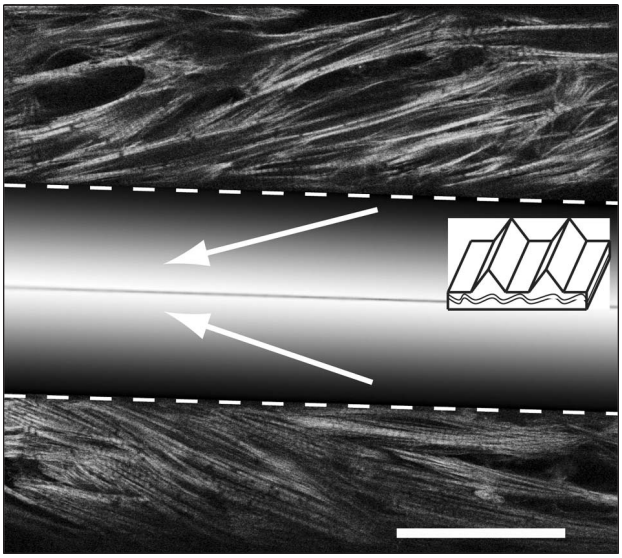

Fig. 2. Bipennate structure of cardiomyocytes grown on G scaffolds. A thin optical (confocal) section from a G scaffold with cardiomyocytes stained for F-actin is shown with a schematic representation of the ridge structure separating the grooves in the middle (boundaries marked by dashed lines). Note the alignment of cytoskeleton at a shallow angle (schematically represented by arrows) to the grooves and the convergence of actin fibers on adjacent grooves mimicking bipennate structures found in skeletal muscle such as *rectus femoralis*. Inset: A schematic diagram of microgrooved scaffold geometry. Scale bar is 50 μm.

Developed engineered tissue bears essential features of the real heart and could serve as a platform for mechanistic studies in cardiac electromechanics, drug testing, and computer model validation.

levels (change in Fura-2 ratio from resting to peak values) and cell length (defined as the distance between two cell borders). Cell strain was then computed as the percent change from resting (diastolic) length and peak (systolic) strain extracted. When cell borders were indistinct, high contrast features (typically intra-cellular inclusion bodies or cellular debris on myocyte surfaces) were used to track motion instead. Statistical analysis was performed using Student's t-test.

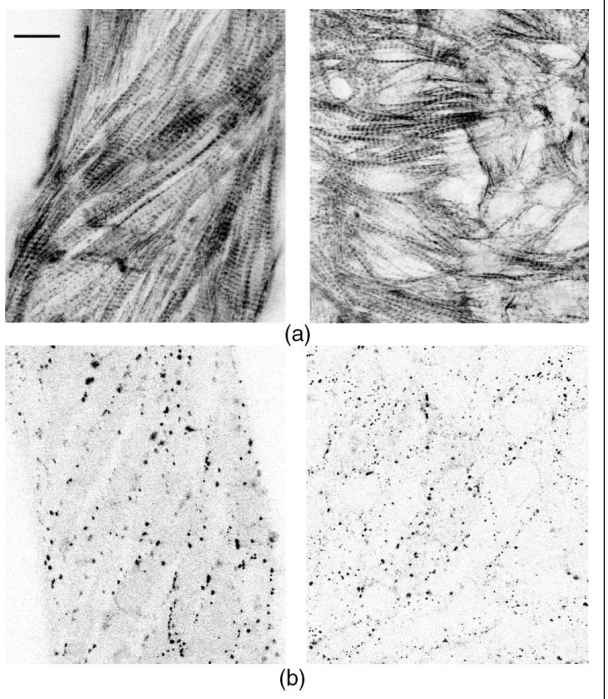

Fig. 3. Cardiomyocytes grown on microgrooved scaffolds (G, left) exhibit profound structural differences compared to flat scaffolds (F, right). (a) Confocal images of F-actin demonstrate highly organized cytoskeleton with well-defined sarcomere structures oriented at a shallow angle relative to the grooves running vertically in (G) scaffolds. (b) Higher density, larger Cx43 clusters are seen in G scaffolds (left) in a typical confocal image of Cx43 compared to F scaffolds (right). Scale bar is 10 μm.

Optical Mapping of Electrical Propagation

A macroscopic CCD system with high numerical aperture was employed to image spatial patterns of electrical propagation in the cardiac constructs (field of view approximately 8 mm in diameter). Cells were stained with a transmembrane potentiometric fluorescent dye, di-8 ANEPPS (Molecular Probes), at 30-50 μM for 5 minutes and epi-illuminated at 535 nm collecting fluorescence at 610 nm. To increase the apparent temporal resolution of the system, cells were chilled to room temperature (21-23 °C). An intensified CCD camera (CCD-72S with Genesys II intensifier, MTI Dage, Michigan City, Indiana) was used to acquire images with 320 x 240 pixels resolution at 60 frames per second (fps).

Specialized automated analysis software (using the Image Processing Toolkit in MATLAB) was developed to handle the large amount of data. The intensity image sequences were cropped and normalized on a pixel-by-pixel basis to saturate the upper and lower 10th percentile over the entire recording time. After baseline correction, each image was binned up to

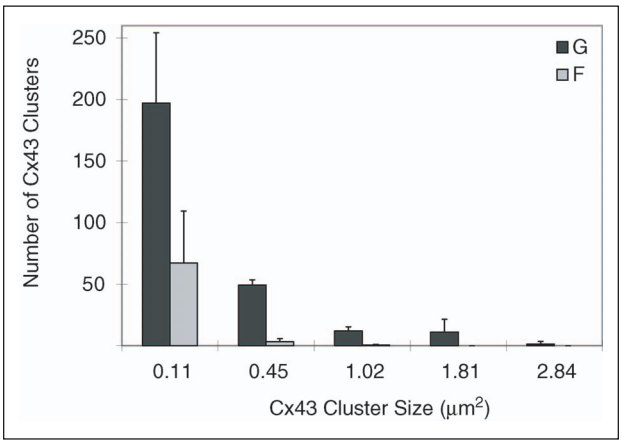

Fig. 4. Quantitative granulometry reveals both increased gap junctional size (no flat scaffolds had gap junctions greater than 1.02 μm^2) and increased numbers of gap junctions. Granulometry involves a combination of morphological operations with increasing element sizes to separate objects of specific sizes. Dividing the number of pixels found in this method by the area of the element size approximates the number of objects having dimensions similar to the shaping element used in the morphological operations. Data shown are mean±SD, n=5 G and n=7 F images were analyzed.

10×10 pixel subregions and spatially (Gaussian) filtered. Activation times were determined by locating the minimum of a Savitzky-Golay filtered first derivative, and isochronal maps were constructed.

Results

The first striking structural difference observed between F and G scaffolds was the peculiar alignment of cells on G scaffolds under phase-contrast microscopy. Cardiomyocytes were seen bridging the grooves under a shallow angle in a pattern reminiscent of bipennate skeletal muscle (fibers converging in a feather-like structure). Confocal imaging confirmed F-actin alignment in a similar arrangement (Figure 2), consistent with nuclear elongation and alignment we have previously reported in cardiomyocytes grown on G scaffolds [5]. At higher magnification, well-developed sarcomeres were visible in both F and G scaffolds [Figure 3(a)]. However, actin cytoskeleton on F scaffolds appeared less mature and more disorganized—never having a bipennate or multipennate structure.

In addition to cytoskeletal changes, augmentation of gap junctional proteins (connexin-43) within the grooves was observed [Figure 3(b)]. Estimation of Cx43 cluster size by granulometry (Figure 4) revealed both an increase in Cx43 density (as demonstrated by increased numbers of Cx43 clusters in each size category) as well as a shift in the relative distribution of cluster sizes favoring larger clusters (as seen by the increased percentage of Cx43 clusters at larger sizes relative to total number of clusters). Together, these data imply that the greater numbers of larger Cx43 clusters was not simply a reflection of increased Cx43 density (in which case the percentage of large Cx43 clusters would have remained the same).

Electromechanical testing was then performed to see if these structural changes resulted in any functional differences. Microscopic recordings demonstrated significantly increased peak systolic intra-cellular calcium levels [$p<0.05$, Figure 5(a)]. Consistent with this finding is the observation of increased cellular strain [$p<0.05$, Figure 5(b)] since intra-cellular calcium concentration is linked to the mechanical performance of the cardiomyocytes. Additionally, spontaneous and persistent synchronized contractions were often observed on G scaffolds as early as day three after plating. Such pacemaking activity can also be seen in the characteristic slow "depolarization" in some calcium transients observed [Figure 5(c)]. In contrast, F scaffolds rarely exhibited such organized and persistent pacemaking behavior and spontaneous contractions.

One of the intents of creating these engineered cardiac constructs was to induce structural and functional anisotropy.

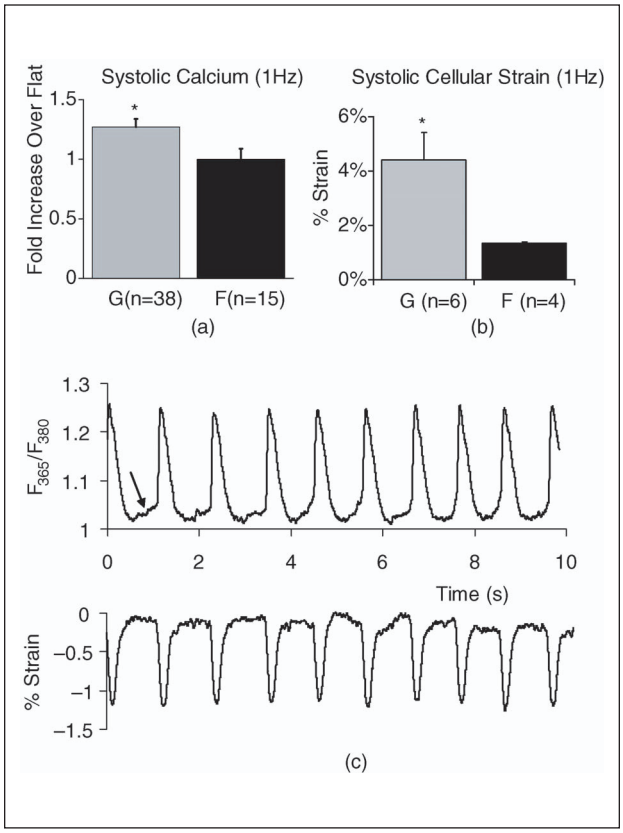

Fig. 5. Optical recordings of functional changes (calcium and strain) in microgrooved samples versus control. (a) Cells grown on microgrooved surfaces (G) have significantly increased systolic calcium levels compared to cells on flat (F) surfaces when field-stimulated at 1 Hz. (b) Increased uni-axial strain of cells on G versus F scaffolds. (c) Example traces of intracellular calcium ratios (top) and mechanical strain (bottom) in spontaneously contracting cells on a G scaffold. Peak (systolic) intracellular calcium concentration is proportional to the ratio of fluorescence at 365 nm (F_{365}) and 380 nm (F_{380}), while mechanical strain is defined as percent change from diastolic (resting) length. Note the slow depolarization characteristic of pacemaking cells (arrow). Data shown are mean±SEM (n is number of examined scaffolds); stars indicate significance at $p<0.05$.

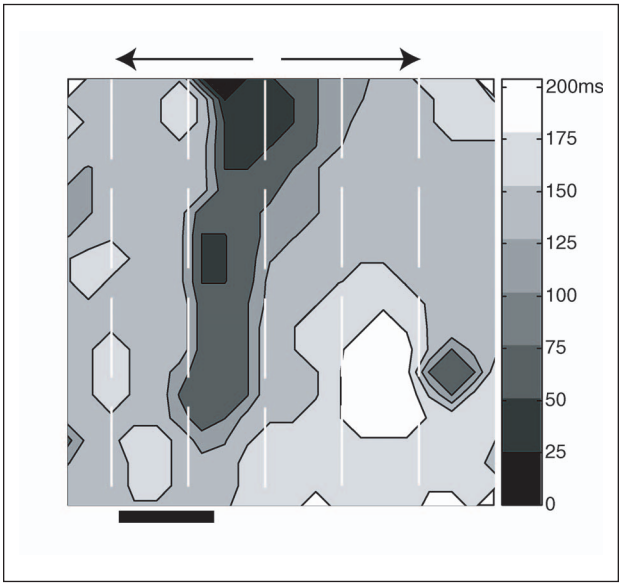

Fig. 6. Cells on grooved surfaces exhibit anisotropic propagation. The activation map shows spontaneous propagation within grooves faster than across grooves. Plotted are times of activation of each location relative to the earliest activation (in this case, at the top center of the image). The action potentials spread laterally to both sides (indicated by the arrows on top) as well as from top to bottom. Orientation of the microgrooves is schematically depicted as dashed white vertical lines (not drawn to scale). Contours indicate isochronal activation times in milliseconds, as shown on the right. Scale bar represents 1 mm.

A low magnification, large-area imaging was performed to assess action potential propagation across microgrooves. Such macroscopic optical mapping revealed highly anisotropic conduction velocities with near instantaneous propagation within the grooves (>10 cm/s) but delayed conduction across the grooves (<2 cm/s, Figure 6) at the lowered temperatures used during imaging of the samples.

Discussion and Conclusions

Anisotropy is an essential feature of cardiac tissue. Previous attempts to mimic it in vitro have employed 2-D micropatterning [6], [7], extracellular matrix manipulations [8], [9], or surface microabrasions [7]. In contrast, our approach involved the introduction of a 3-D microenvironment and resulted in some interesting structural characteristics (bipennate arrangement). Functionally, the engineered constructs exhibited extreme levels of anisotropy, which could be well controlled in our system by the spatial features in the master template. The chosen approach to engineer a model cardiac tissue also brought about significant functional changes (in calcium and strain levels), possibly attributable to 3-D effects in cell attachment and subsequently altered mechanical environment. Thus, developed engineered tissue bears essential features of the real heart and, combined with the optical mapping tools reported in this article, could serve as a platform for mechanistic studies in cardiac electromechanics, drug testing, computer model validation, and investigation of cell-scaffold responses for tissue engineering and tissue regeneration purposes.

Harold Bien received the B.S. degree in biomedical engineering, materials science and engineering, and biology from Johns Hopkins University, Baltimore, Maryland, in 1999. He is currently a M.D./Ph.D. student in biomedical engineering at Stony Brook University, researching a 3-D model of engineered cardiac tissue using optical mapping methods. He is a member of the IEEE and the IEEE Engineering in Medicine and Biology Society (EMBS).

Lihong Yin received the B.S. degree in chemical engineering and international enterprise management from the Dalian University of Technology, Dalian, China, in 2001. She is currently pursuing the M.S. degree in biomedical engineering at Stony Brook University, Stony Brook, New York. Her thesis focuses on frequency-dependent changes in calcium handling in cardiac tissue and time-frequency analysis.

Emilia Entcheva received the B.S./M.S. degree in electrical engineering from the Technical University – Sofia, Bulgaria, in 1988 and the Ph.D. degree in biomedical engineering from The University of Memphis, Memphis, Tennessee, in 1998. After a postdoctoral fellowship at Johns Hopkins University, Baltimore, Maryland, in 2001 she became an assistant professor in biomedical engineering, physiology, and biophysics at Stony Brook University, Stony Brook, New York. Her research interests include engineering functional cardiac tissue in the lab using microfabrication, elastic and biodegradable polymers; developing optical techniques and algorithms for the mapping of electrical and mechanical activity in the obtained tissue equivalents; and computer modeling in cardiac electrophysiology.

Address for Correspondence: Harold Bien, Dept. of Biomedical Engineering, Stony Brook University, HSC T18-030, Stony Brook, NY 11794-8181 USA. Phone: +1 631 444 1498. Fax: +1 631 444 6646. E-mail: hbien@jhu.edu.

References

[1] R.E. Akins, "Can tissue engineering mend broken hearts?" *Circ. Res.*, vol. 90, no. 2, pp. 120-122, 2002.

[2] D.D. Streeter, "Gross morphology and fiber geometry of the heart," in *Handbook of Physiology,* R.M. Berne, N. Sperelakis, and S.R. Geiger Eds. Bethesda, MD: American Physiological Society, 1979, pp. 61-107.

[3] E. Entcheva, S.N. Lu, R.H. Troppman, V. Sharma, and L. Tung, "Contact fluorescence imaging of reentry in monolayers of cultured neonatal rat ventricular myocytes," *J. Cardiovasc. Electrophysiol.*, vol. 11, no. 6, pp. 665-76, 2000.

[4] E. Entcheva, H. Bien, and E. Tchernev, "Acoustic micromachining for controlled cell growth," presented at Fourth Annual BioMEMS and Biomedical NanoTech World Conference, Washington, DC, 2003.

[5] E. Entcheva and H. Bien, "Tension development and nuclear eccentricity in topographically controlled cardiac syncytium," *J. Biomed. Microdev.*, vol. 5, no. 2, pp. 165-170, 2003.

[6] S. Rohr, D. Shoelly, and A.G. Kleber, "Patterned growth of neonatal rat heart cells in culture. Morphological and electrophysiological characteristics.," *Circ. Res.*, vol. 68 pp. 114-130, 1991.

[7] N. Bursac, K.K. Parker, S. Iravanian, and L. Tung, "Cardiomyocyte cultures with controlled macroscopic anisotropy: a model for functional electrophysiological studies of cardiac muscle," *Circ. Res.*, vol. 91, no. 12, pp. e45-e54, Dec. 2002.

[8] D.G. Simpson, L. Terracio, M. Terracio, R.L. Price, D.C. Turner, and T.K. Borg, "Modulation of cardiac myocyte phenotype in vitro by the composition and orientation of the extracellular matrix," *J. Cell. Physiol.*, vol. 161, no. 1, pp. 89-105, 1994.

[9] V. Fast, B. Darrow, J. Saffitz, and A. Kleber, "Anisotropic activation spread in heart cell monolayers assessed by high-resolution optical mapping. Role of tissue discontinuities," *Circ. Res.*, vol. 79, pp. 115-127, 1996.